Volume 12 Number18
Journal of Advances in chemistry

Optimum Design of Shell and Tube Heat Exchanger Using Artificial Immune System Approach

K.Vetrivel Kumar, M.Saravanan
Associate professor, SCAD institute of Technology, Palladam, Tamil Nadu, India.
vetrivelkumark@gamil.com
Head & Professor, SSM Institute of Engineering and Technology,Dindigul,Tamil Nadu, India.
drmsaravanan@yahoo.com

ABSTRACT

This paper presents the economic optimization of shell and tube heat exchangers design approach through an artificial immune system algorithm for minimizing the cost. Since complex geometric parameters, with thermodynamic and fluid dynamic factors, consume more time and offer a minimum possibility for an optimum result in the case of conventional design, the design process becomes difficult. The proposed algorithm provides the designer with an optimum solution in less amount of time by analyzing three different case studies. Three design variables such as shell internal diameter, tube outer diameter and baffle spacing from the different design parameters are taken into account for this optimization. The results are weighed against those obtained by various researchers.

Keywords

Shell and tube heat exchanger, Artificial Immune System, Economic optimization

Academic Discipline And Sub-Disciplines

Mechanical Engineering and equipement design

SUBJECT CLASSIFICATION

Heat tranasfer equipment design and optimization

TYPE (METHOD/APPROACH)

The Artificial Immune System optimation technique is used to economic design of a shell and tube heat exchenger and compared to other optimization techniques.

INTRODUCTION

Heat exchanger is a device built to transfer heat from hot fluid to cold fluid. Apart from the various types of heat exchangers, Shell and Tube Heat Exchangers (STHEs) are popularly used in various industries such as process industries, refrigeration, power plants, power condensers, oil coolers, chemical and petroleum industries as shown in fig.1. The design of STHEs is a complex process as it includes thermodynamic and fluid dynamic design, cost estimation and optimization. The designer should have experience in various fields to design an optimum STHE [6-8].

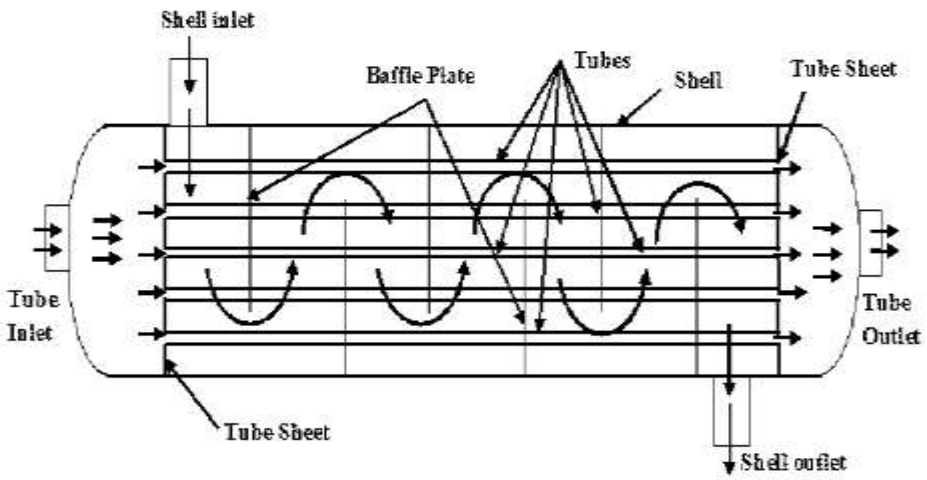

Fig.1. Typical diagram of shell and tube heat exchanger (one tube and one shell pass)

The heat exchanger fulfills the heat duty requirement with optimum design. To design new equipment, reference geometric configurations of the equipment and the permissible pressure drop have to be fixed. Then, to define the new design parameters, the design specifications and the assumption of numerous mechanical and thermodynamic parameters are considered. The pressure drop and heat transfer rates are inter-reliant responsibilities on STHEs and influence the design. The designer's choices are verified based on iterative procedures involving many trials until a reasonable design is obtained [1, 9].

When the designer is free to select the pressure drop, an economic analysis can be made to determine the exchanger design which gives the lowest operating costs, taking into consideration both capital and pumping costs. However, a full economic analysis is sensible for very large, expensive, exchangers [2]. Due to the important role of STHEs in industries, there are several earlier studies on the optimization of heat exchangers. Numerous investigators have used to sort the optimum parameters of STHEs with the help of various optimization techniques for different objective functions. The optimization procedure involves selection of the major geometric parameters such as baffle spacing, baffle cut, number of tubes, internal and external diameter of shell and tube, types of head, length of the exchanger, tube layout, allocation of fluid, pressure drop in both shell and tube side. The selection methods of geometric and operational parameters are typically recommended by design codes [8]. Graphical analysis of the search space [11], mixed integer nonlinear programming [12, 13], systematic screening of tube count tables [14, 15], Simulated Annealing Algorithm (SAA) is done to optimize the heat transfer area and overall cost [16]. Some studies are based on artificial intelligence techniques for optimization of shell and tube heat exchangers. Genetic Algorithm (GA) is used to determine the optimum design variables of STHEs considering pressure drop as constraint and cost estimation as objective function [6, 17]. Differential Evolution (DE) is applied to estimate the optimal heat transfer area and overall cost through optimal design parameters of STHEs [17] where as Particle Swarm Optimization (PSO) minimizes total annual cost by achieving optimal design parameters of STHEs[19]. While a single parameter like baffle spacing is taken into consideration in some cases [21,22,23] others optimized a variety of operational and geometrical parameters. A procedure to minimize the total cost of the equipment, including capital investment and the sum of discounted annual energy expenditures related to pumping; by employing a genetic algorithm, is proposed for optimal design of shell and tube heat exchangers.

As seen above literature, the Artificial Immune System (AIS) is not found in the design and optimization of shell and tube heat exchanger. Three case studies specifying significant cost reductions with respect to traditionally designed exchangers are taken into consideration for demonstrating the effectiveness and accuracy of the proposed algorithm. The results, which are previously published, obtained by various other optimization techniques are compared with the results of the proposed algorithm to prove its effectiveness for the same objective function. This study also points out the influencing parameters of STHEs for economically optimized design.

2. Overview of Artificial Immune System (AIS) Algorithm

In the past few years, researchers showed great interest in studying nontraditional optimization techniques inspired by nature that gained popularity in the field of combinational optimization. AIS is one such technique inspired by the immune system of our body. Some of the important systems are DNA computation, artificial neural networks, artificial immune systems and evolutionary computation [21,23]. The immune system is a compound of cells, molecules and organs which can perform various tasks, like recognition of pattern, learning, generation of diversity, noise tolerance, generalization, memory acquisition, optimization, uniqueness, recognition of foreigners, anomaly detection, distributed detection, imperfect detection and distributed detection.

AIS refers to a computational system influenced by theoretical immunology and observed principles, functions and models of immune that is used to solve engineering problems. The latest research works show the extensive usage of AIS in optimization, scheduling, anomaly detection, computer and its network security, pattern recognition and data mining [20, 37-39]. The effective mechanisms of an immune system, which are the clonal selection, learning ability, memory, robustness and flexibility make artificial immune systems useful for engineering problems. The proposed AIS is built on the clonal selection and affinity maturation principles.

The objective of the immune system is to protect human body from attacks by foreign organisms called antigens. The immune cells, antibodies, produced because of the intrusion of foreign organisms are able to recognize antigens and will increase rapidly in number through cloning. This process is called the clonal selection principle. A clone is the offspring cell that is the identical copy of parent cell [15].

Affinity maturation is the process of mutation and selection of the variant offspring that accurately recognizes the antigen. The two basic mechanisms of affinity maturation are mutation and receptor editing. The mutation process causes structural changes in the cells and these changes may increase the affinity of the antibody. The immune system preserves these high affinity offspring cells. Owing to the cloning and mutation process, the affinity of the antibodies improved which results in antigen elimination. Due to the random nature of the mutation process, a large proportion of mutating genes become nonfunctional. These nonfunctional cells are deleted and are replaced with new receptors. This process is called receptors editing. The important features of AIS are recognition, variation, learning, memory, distributed perception and self-organizing. These features make AIS more superior than GA or any other method [15]. The main objective of AIS is to solve complex computational problems such as pattern recognition, optimization and elimination. This is an important difference between AIS and theoretical immune systems, when the first one is dedicated primarily to computing, the later one is subjected to the modelling of the immune system in order to recognize its behavior. The use of combination of the above approaches of the immune systems has resulted in the improvement of AIS [16].

In this work, AIS algorithm has been proposed to achieve optimal design of STHE. The general AIS algorithm consists of the following steps:

Step 1: ***Initialization:*** it refers to a creation of a random population of individuals, "P".

Step 2: ***Affinity evaluation:*** it is an evaluation where the affinity of each individual in the population is measured using:

$$Affinity = \frac{1}{Objective\ Function\ Value}$$

Step 3: ***Clonal selection:*** The n best individuals of the population based on the affinity measure are selected in this process.

Step 4: ***Clonal expansion:*** As the name suggests, it clones the n best individuals of the population, proportional to the rate of cloning. The clone means an identical copy of the original string. (The clone size is an increasing function of the affinity measure.)

Step 5: ***Affinity maturation*:** It Mutates each clone to generate a matured antibody of the population and preserves the improved individuals for the next generation.

Step 6: ***Meta dynamics:*** Here, R individuals with low affinity value with randomly generated new ones are replaced. The lower the affinity of cells, the higher is the probability of being replaced. This process introduces diversity into the population.

Step 7: ***Cycle:*** Step 2 to step 6 are repeated until the criteria is met.

The flowchart of the heat exchanger designing procedure is given in Fig.3.

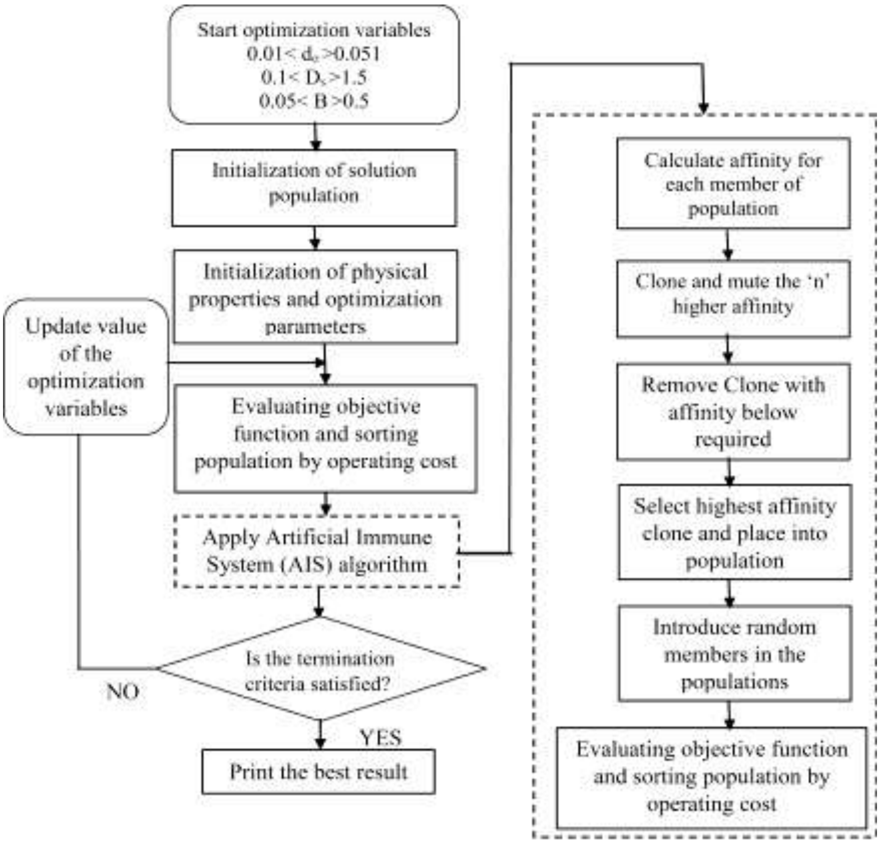

Fig.3. Flowchart of AIS approach in shell and tube heat exchanger design procedure

3. Mathematical models

3.1. Heat exchanger design formulations-Heat transfer coefficient

3.1.1 Shell side Heat transfer coefficient

The shell side heat transfer coefficient (h_s) of the segmental baffled shell and tube heat exchanger is computed from the following Kern's formulation [9].

$$h_s = 0.36 \frac{k_s}{D_e} \mathrm{Re}_s^{0.55} \mathrm{Pr}_s^{1/3} \left(\frac{\mu_t}{\mu_w} \right)^{0.14} \quad (1)$$

Where D_e denotes shell hydraulic diameter computed as [2, 9]

$$D_e = \frac{4\left(Pt^2 - \frac{\pi d^2}{4}\right)}{\pi d_o} \quad for\ square\ pitch \quad (2)$$

$$D_e = \frac{4(0.43Pt^2 - \frac{0.5\pi d_o^2}{4})}{0.5\pi d_o} \quad for\ triangular\ pitch \quad (3)$$

Where Re_s is the shell side Reynolds number and is computed from the following formulation

$$\mathrm{Re}_s = \frac{m_s D_e}{A_s \mu_s} \qquad (4)$$

A_s is cross sectional area normal to the flow direction and determined by [2, 9]

$$A_s = \frac{D_s BC}{Pt} \qquad (5)$$

Where C is clearance,

$$C = Pt - d_o \quad (6)$$

The flow velocity for shell side can be obtained from (7)

$$v_s = \frac{m_s}{\rho_s A_s} \qquad (7)$$

Prandtl number for shell side is computed from (8)

$$\mathrm{Pr}_s = \frac{\mu_s Cp_s}{k_s} \qquad (8)$$

3.1.2 Tube side Heat transfer coefficient

The tube side heat transfer coefficient (h_t) is calculated from the following relationship[17].

$$h_t = \frac{k_t}{d_i}\left[3.657 + \frac{0.677\left(\mathrm{Re}_t\,\mathrm{Pr}_t\,\frac{d_i}{L}\right)^{1.33}}{1 + 0.1\mathrm{Pr}_t\left(\mathrm{Re}_t\,\frac{d_i}{L}\right)^{0.3}}\right] \qquad (9)$$

(If $Re_t < 2300$)

$$h_t = \frac{k_t}{d_i}\left\{\frac{\frac{f_t}{8}(\mathrm{Re}_t - 1000)\mathrm{Pr}_t}{1 + 12.7\sqrt{\frac{f_t}{8}}\left(\mathrm{Pr}_t^{0.67} - 1\right)}\left[1 + \left(\frac{d_i}{L}\right)^{0.67}\right]\right\} (10)$$

(If $2300 < Re_t < 10{,}000$)

$$h_t = 0.027\frac{k_t}{d_i}\mathrm{Re}_t^{0.8}\,\mathrm{Pr}_t^{1/3}\left(\frac{\mu_t}{\mu_w}\right)^{0.14} \qquad (11)$$

(If $Ret > 10{,}000$)

Where f_t is the Darcy friction factor [17]

$$f_t = \left(1.82.\log_{10}\mathrm{Re}_t - 1.64\right)^{-2} \qquad (12)$$ Also $d_i = 0.8\, d_o$

Reynolds number of tube side (Re_t) is calculated by

$$\mathrm{Re}_t = \frac{\rho_t\, v_t\, d_i}{\mu_t} \qquad (13)$$

Flow velocity for tube side is found by

$$v_t = \frac{m_t}{\left(\frac{\pi}{4}\right) d_t^2\, \rho_t}\left(\frac{n}{N_t}\right) \qquad (14)$$

Where n is the number of tube passes and N_t is the number of tubes. N_t is determined by the following correlation (15) [1-3, 5]

$$N_t = C1\left(\frac{D_s}{d_o}\right)^{n1} \qquad (15)$$

Where C1 and n_1 are constant values that are selected according to number of passes and tubes arrangement as exhibited in table 1 for different flow arrangements as shown in Fig.2. [2].

Pr_t is the tube side Prandtl number and expressed by

$$\mathrm{Pr}_t = \frac{\mu_t\, Cp_t}{k_t} \qquad (16)$$

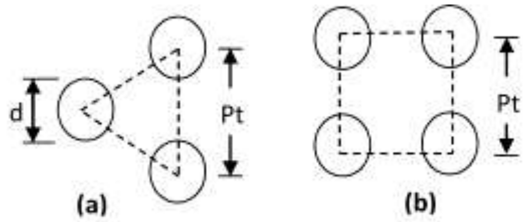

Fig.2.Tube pitch arrangements a) Triangular b) Square

3.1.3 Calculate overall heat exchanger surface area (A) and tube length (L)

The overall heat exchanger surface area (A) is computed using Log Mean Temperature Difference (LMTD) approach.

$$A = \frac{Q}{U\, F\, LMTD} \qquad (17)$$

The overall heat transfer coefficient (U) is found by using the following equation [2, 9]

$$U = \frac{1}{\frac{1}{h_s} + R_{fs} + \frac{d_o}{d_i}\left(R_{ft} + \left(\frac{1}{h_t}\right)\right)} \qquad (18)$$

The fouling resistances are assigned for the flow configuration based on fluid type and operating temperature [1, 4, 15]. The temperature difference correction factor [2] is calculated from the following equation,

$$F = \frac{\sqrt{R^2+1}}{R-1}\,\frac{\ln\left(\frac{1-P}{1-PR}\right)}{\ln\left[\frac{2-P\left(R+1-\sqrt{R^2+1}\right)}{2-P\left(R+1+\sqrt{R^2+1}\right)}\right]} \qquad (19)$$

Where R refers to the correction coefficient that is given by

$$R = \frac{Ti_s - To_s}{To_t - Ti_t} \qquad (20)$$

and P is the efficiency which is specified by

$$P = \frac{To_t - Ti_t}{Ti_s - Ti_t} \qquad (21)$$

The heat transfer rate is given for sensible heat transfer by

$$Q = m_s\, Cp_s (Ti_s - To_s) = m_t\, Cp_t (Ti_t - To_t) \qquad (22)$$

Table 1 Values of C1 and n_1 coefficients

No.of passes	Triangular tube pitch Pt = 1.25d_o		Square tube pitch Pt = 1.25d_o	
	C1	n_1	C1	n_1
1	0.319	2.142	0.215	2.207
2	0.249	2.207	0.156	2.291
4	0.175	2.285	0.158	2.263
6	0.0743	2.499	0.0402	2.617
8	0.0365	2.675	0.0331	2.643

3.2 Pressure drop

The pressure drop allowance in heat exchanger attributes to the static fluid pressure that can be expended to drive the fluid through the exchanger. Generally, heat exchangers possess adjacent physical and economical affinity between heat transfer and pressure drop. To maintain a constant heat capacity in the heat exchanger that is to be designed, an increase in the flow velocity leads to a rise in heat transfer coefficient which results in compact exchanger design and lower investment cost. Moreover, increase in flow velocity produces higher pressure drop in heat exchanger resulting in additional running cost. Hence, it is essential to consider along with heat transfer coefficient while designing a heat exchanger and the best solution for the system must be found.

The tube side pressure drop is calculated by taking into account the sum of the pressure spread along the tube length and concentrated pressure losses in elbows and in the inlet and outlet nozzles [9]

$$\Delta P_t = \Delta P_{tube\ length} + \Delta P_{tube\ elbow} = \frac{\rho_t v_t^2}{2}\left(\frac{L}{d_i} f_t + p\right) n \qquad (23)$$

p is a constant and different values are assigned by different authors. Kern [9] assumed *p* =4, while Sinnot et al [2] assumed *p* =2.5

The shell side pressure drop is [9, 17]

$$\Delta P_s = f_s \left(\frac{\rho_s v_s^2}{2}\right)\left(\frac{L}{B}\right)\left(\frac{D_s}{D_e}\right) \qquad (31)$$

The friction factor f_s is obtained by using:

$$f_s = 2b_o \operatorname{Re}_s^{-0.15} \qquad (32)$$ and

b_o= 0.72 [18] valid for Re_s<40,000

The equation that considers pumping efficiency (η) to compute pumping power is given below:

$$P = \frac{1}{\eta}\left(\frac{m_t}{\rho_t}\Delta P_t + \frac{m_s}{\rho_s}\Delta P_s\right) \qquad (33)$$

3.3. Objective function

To find the optimal design of the shell and tube heat exchanger, an economical design considers several technical variants. The Total cost C_{tot} is considered as the objective function that includes capital investment (C_i), energy cost (C_e), annual operating cost (C_o) and total discounted operating cost (C_{oD})[17]

$$C_{tot} = C_i + C_{oD} \qquad (34)$$

The capital investment C_i is taken into account as a function of the exchanger surface adopting Hall's correlation [14]

$$C_i = a_1 + a_2 A^{a3} \qquad (35)$$

Where a_1= 8000, a_2= 259.2, a_3= 0.91 for exchangers made with stainless steel for both shell and tubes [41]

The following equations helps to compute discounted operating cost associated with pumping power to overcome friction losses:

$$C_{oD} = \sum_{k=1}^{n_y} \frac{C_0}{(1+i)^k} \qquad (36)$$

$$C_o = P C_E H \qquad (37)$$

Considering the calculations above, the total cost is calculated from equation (34). The process is continued for computing the new value of exchanger surface area (A), exchanger length (L), total cost (C_{tot}) and an equivalent optimal exchanger design specifications. On every occasion, the optimization algorithm tends to change the values of the design variables d_o, D_s, and B to minimize the objective function.

The following upper and lower bounds for the optimization variables are instituted such as shell internal diameter (D_s) ranging between 0.1m and 1.5m, baffle spacing (B) ranging between 0.05m and 0.5m and tube outside diameter (d_o) ranging between 0.015m and 0.051m. The values of all the discounted operating costs are computed with ny = 10 yr, annual discount rate (i) = 10%, energy cost (C_e) = 0.12 €/kW h and annual amount of work hour H= 7000yr/h.

4. Results and discussion

Three cases are considered from literature to check the effectiveness and validity of the recommended approach and the results have reliable reference sizing data for the sake of comparison. The following three different cases are considered to represent a wide range of possible applications.

Case-1: methanol-sea water exchanger, 4.34 (MW) duty [2]

Case 2: kerosene-crude oil exchanger, 1.44 (MW) duty [9]

Case 3: distilled water- raw water exchanger, 2.09(MW) duty [2]

For every case mentioned above, the input to the described AIS algorithm is provided based on the original design specifications that are displayed in table 2. The result of the optimal design of exchanger obtained by AIS proposed algorithm is compared with the results obtained by Caputo et al. [17] who applied GA approach, Patel et al.[19] PSO approach, Sahin et al[17] ABC algorithm, Hadidi et al.[18] BBO approach and with original design solution specified by Sinnot et al.[2] and Kern [9] (shown in Tables 3,4,5). In order to allow a consistent comparison, cost functions of all three approaches are computed as described in Section 3.3 and all the values related to cost are taken from the work of Caputo et al. [9] who attempted all the case studies by GA approach.

Table 2: Design specifications for different case studies [17]

	m (kg/s)	T_i (°C)	T_i (°C)	ρ (kg/m³)	Cp (kJ/kg.K)	μ (Pa.s)	K (W/mK)	R_f (m²K/W)
Case-1								
Shell side: Methanol	27.80	95.00	40.00	750	2.84	0.00034	0.19	0.00033
Tube side: Sea water	68.90	25.00	40.00	995	4.20	0.00080	0.59	0.00020
Case-2								
Shell side: Kerosene	5.52	199.00	93.30	850	2.47	0.00040	0.13	0.00061
Tube side: Crude oil	18.80	37.80	76.70	995	2.05	0.00358	0.13	0.00061
Case-3								
Shell side: Distilled water	22.07	33.90	29.40	995	4.18	0.00080	0.62	0.00017
Tube side: Raw water	35.31	23.90	26.70	999	4.18	0.00092	0.62	0.00017

4.1. Case 1: Methanol-sea water exchanger, 4.34 (MW) duty

The original design assumed as an exchange with one shell side passage and two tube side passages with triangle pitch pattern is maintained in the present approach. Methanol acts as hot fluid and brackish water is the cold fluid. The results in Table 3 show that a significant increase in the number of tubes reduces the tube side flow velocity consecutively reducing tube side heat transfer coefficient. The reduction in shell diameter increases the shell side flow velocity and shell side heat transfer coefficient. The effect of higher shell side heat transfer coefficient increases the overall heat transfer coefficient and thereby reduces heat exchanger area and heat exchanger length in the case of AIS as compared to other algorithms. The capital investment is also decreased because of reduction in heat exchanger area.

The tube side heat transfer coefficient is reduced due to the decrease in Reynolds number which is varied based on the tube side velocity and tube internal diameter. The tube outer diameter diminishes to reduce the tube internal diameter which influences Reynolds Number. The tube side velocity is reduced by increasing the number of tubes. The tube side heat transfer coefficient is decreased by 33% (Original design), 31.3% (GA), 29.8 % (PSO), 33.2% (ABC), and 50.5% (BBO). The reduction in equivalent diameter induces to reduce the shell side Reynolds number and increases shell side heat transfer coefficient. The shell side heat transfer coefficient is increased by 72.1% (Original design), 69.2% (GA), 65.4% (PSO), 39.8% (ABC), and 61.1 % (BBO). The increment in overall heat transfer coefficient is 26.6 % (Original design), 21.2% (GA), 14.8% (PSO), and 0.7 %(ABC), 9.9% (BBO).

Fig.4. Total cost in various algorithms (Case 1)

The reduction in tube side flow velocity reduces the tube side pressure drop while the lower shell side flow velocity decreases the shell side pressure drop, which in turn decreases the annual pumping cost by 62.7% (Original design), 16.9% (GA), 24.2% (PSO), 22.5% (ABC) and 20.1 % (BBO). It represents the combined effect of capital investment and operating costs that has lead to a reduction in the total cost. The total cost value is reduced by 22.8 % in the case of Artificial immune system (AIS) algorithm compared to original design and also reduced by 9.9%(GA), 6.4 %(PSO),1.9 %(ABC) and 1.5 %(BBO) respectively. Fig.4. describes the cost comparison of literature, genetic algorithm, particle swarm optimization, artificial bee's colony, and biogeography based optimization, artificial immune system.

4.2. Case 2: Kerosene - crude oil exchanger, 1.44 (MW) duty

In this case, kerosene and crude oil are used as hot and cold fluid respectively in the corresponding shell side and tube side heat exchanger. This heat exchanger comprises of four tube side passages coupled with a square pitch pattern and a shell side passage. This case results are shown in table 4, the tube side heat transfer coefficient has a direct deviation with tube side flow velocity. Similarly, the shell side heat transfer coefficient has a direct deviation with shell side flow velocity. Hence, the increase of the overall heat transfer coefficient is due to the combined increment in tube side and shell side heat transfer coefficient which reduces heat exchanger area and heat exchanger length in the case of AIS as compared to other algorithms. Both the tube side and shell side heat transfer coefficients are decreased according to reduction in Reynolds number effected by the diminution in tube side outer diameter and velocity. The tube side velocity diminishes when the numbers of tubes are increased. On comparison, overall heat transfer coefficient is enhanced by 4.5% (Original design), 2.7 % (ABC), 4.3 % (BBO) and diminishes by 13.3% (GA), 23.3% (ABC).

Increment in number of tubes decreases tube side velocity and tube length. It signifies the decrement in the tube side pressure drop. The shell diameter is increased by 59.5% compared to the original design. Compared to other approaches, it is higher by 52.2% (GA), 55.27% (PSO), 75.03% (ABC), and 43.8% (BBO) respectively. It is found to decrease shell side velocity which causes decrease in shell side pressure drop. The capital investment is also decreased because of reduction in heat exchanger area. The decrement in both tube side and shell side pressure drop leads to reduction in annual pumping cost. The combined effect of capital investment and operating costs reduces the total cost. Total cost value of Artificial Immune System (AIS) algorithm is reduced by 28.8 % (Original design) 5.2 % (GA), 3.4% (PSO), 4.8% (ABC) and 2.8% (BBO). Fig.5. presents the cost comparison of present approach and other approaches.

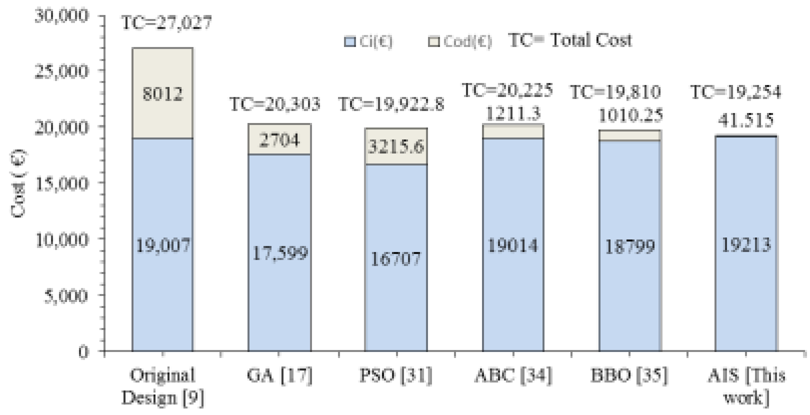

Fig.5. Total cost in various Algorithms (case 2)

4.3. Case 3: Distilled water- raw water exchanger, 2.09 (MW) duty

In this case, distilled water and raw water are used as hot fluid and cold fluid respectively in corresponding shell side and tube side. This heat exchanger includes two tube side passages plus a triangle pitch pattern and one shell side passage. The results, given in table 5, show that Reynolds number decreases due to decrement of tube internal diameter and tube side flow velocity. Flow velocity diminishes while increasing the number of tubes which in turn leads to reduce the tube side heat transfer coefficient. Enriched shell diameter and compacted baffle spacing influence shell side pass area increment. The increase in shell side pass area leads to reduce shell side flow velocity and Reynolds number. The above denoted parameters influence shell side heat transfer coefficient decrement. In comparison, heat exchanger surface area is reduced by 15.6% (Original design), 55% (GA), 46.9% (PSO), 35.8% (ABC), and 38.3% (BBO). This has its impact on exchanger length in the case of AIS as compared to other algorithms. The capital investment also decreases due to reduction in heat exchanger area.

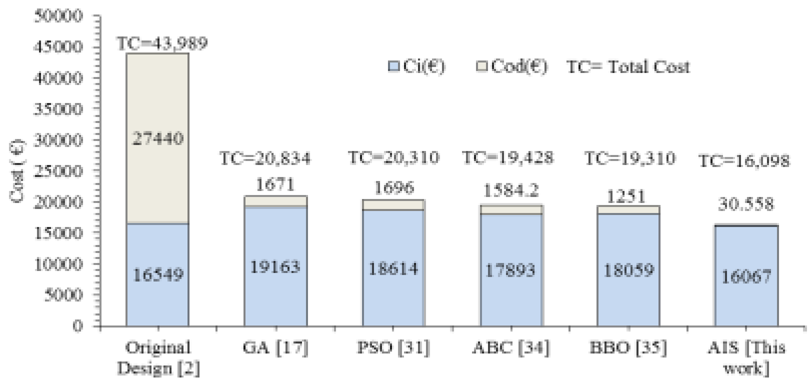

Fig.6. Total cost in various Algorithms (case 3)

The reduction in tube side flow velocity, tube length and internal tube diameter induces decrement of tube side pressure drop. The reduced shell side flow velocity, baffle spacing, tube length, enhanced shell diameter and shell hydraulic diameter decrease shell side pressure drop which increases the annual pumping cost. The combined effect of capital investment and operating cost reduces the total cost. The total cost value with artificial immune system (AIS) algorithm is reduced by 63.4% (Original design), 22.7 %(GA), 20.7 %(PSO), 17.1 % (ABC) and 16.6 % (BBO).Fig.6.illustrates the comparison of cost of the current approach and other methods.

5. Conclusion

Advanced optimization tools are highly instrumental in identifying the complex task of designing the best and cheapest heat exchanger for a specific purpose. This work proposes a solution method of the shell and tube heat exchanger design optimization problem based on the utilization of an Artificial Immune System (AIS).

Based on proposed method, three test cases are solved by the completely developed computer code (Microsoft visual studio C#). The reduction of capital investment and savings in operating costs lead to overall decrease in total cost. Further, with reference to the available literature, the potential improvement of the proposed method is established. Furthermore, AIS technique endorses a rapid solution of the design problem and helps to examine a number of alternative solutions with good quality, giving the designer ample freedom in the final choice with respect to traditional methods. AIS technique's ability is demonstrated using different literature cases and it is found to be accurate and quick with respect to traditional algorithms method. The algorithm proposed here can help the manufacturer and engineers to optimize heat exchangers for engineering applications.

Table 3: Total Cost in methanol - brackish water heat exchanger (Case 1)

	Original design	GA	PSO	ABC	BBO	AIS
D_S (m)	0.894	0.83	0.81	1.3905	0.801	0.869
d_o (m)	0.02	0.016	0.015	0.0104	0.010	0.0158
B (m)	0.356	0.5	0.424	0.4669	0.500	0.4473
N_t	918	1567	1658	1528	3587	1726.49
v_t (m/s)	0.75	0.69	0.67	0.36	0.77	0.639
R_{et}	14,925	10,936	10,503	-	7642.497	10,054.1
P_{rt}	5.7	5.7	5.7	-	5.7	5.7
h_t (W/m^{2}k)	3,812	3,762	3721	3818	4314	2865.7
s_t (m)	0.025	0.020	0.0187	-	0.0125	0.011246
L (m)	4.83	3.379	3.115	3.963	2.040	2.418
Δp_t (Pa)	6,251	4,298	4,171	3043	6156	4071.02
f_t	0.028	0.031	0.0311	-	0.034	0.0313
a_s (m$^{2)}$	0.032	0.0831	0.0687	-	0.0801	0.08
d_e (m)	0.014	0.011	0.0107	-	0.007	0.0112
v_s (m/s)	0.58	0.44	0.53	0.118	0.46	0.4767
Re_s	18,381	11,075	12,678	-	7254.007	10,089
P_{rs}	5.1	5.1	5.1	-	5.1	5.08
h_s (W/m^{2}k)	1573	1573	1,950.8	3396	2197	5643
f_s	0.33	0.357	0.349	-	0.379	0.352
Δp_s (Pa)	35,789	13,267	20,551	8390	13,799	14,564
U (W/m^{2}k)	615	660	713.9	832	755	837.95
A (m^2)	278.6	262.8	243.2	-	229.95	207.25
C_i (€)	51,507	49,259	46,453	44,559	44,536	44,980
C_o (€/yr)	2,111	947	1,038	1014.5	984	787.06
C_{od} (€)	12,973	5,818	6778.2	6233.8	6046	4836.144
C_{total} (€)	64,489	55,077	53,231	50,793	50,582	49,816.7

Table 4: Total Cost in kerosene and crude oil heat exchanger (Case 2)

	Original design	GA	PSO	ABC	BBO	AIS
D_S (m)	0.539	0.63	0.59	0.3293	0.74	1.319
d_o (m)	0.025	0.02	0.015	0.0105	0.015	0.0165
B (m)	0.127	0.12	0.1112	0.0924	0.1066	0.220
N_t	158	391	646	511	1061	3184

v_t (m/s)	1.44	0.87	0.93	0.43	0.69	0.17
Re_t	8227	4068	3283	-	2298	635.84
P_{rt}	55.2	55.2	55.2	-	55.2	55.2
h_t (W/m^{2}k)	619	1168	1205	2186	1251	132.25
s_t (m)	0.031	0.025	0.0187	-	0.0188	0.018
L (m)	4.88	2.153	1.56	3.6468	1.199	0.84
Δp_t (Pa)	49,245	14,009	16926	1696	5109	184.66
f_t	0.033	0.041	0.044	-	0.05	0.046
a_s (m$^{2)}$	0.0137	0.0148	0.0131	-	0.0158	0.0148
d_e (m)	0.025	0.019	0.0149	-	0.0149	0.016
v_s (m/s)	0.47	0.43	0.495	0.37	0.432	0.11
Re_s	25,281	18,327	15844	-	13689	12876
P_{rs}	7.5	7.5	7.5	-	7.5	7.6
h_s (W/m^{2}k)	920	1034	1288	868	1278	90.22
f_s	0.315	0.331	0.337	-	0.345	0.41
Δp_s (Pa)	24,909	15,717	21745	10667	15275	13879
U (W/m^{2}k)	317	376	409.3	323	317.75	332
A (m^2)	61.5	52.9	47.5	61.56	60.35	57.44
C_i (€)	19.007	17,599	16707	19014	18799	19213
C_o (€/yr)	1304	440	523.3	197.13	164.4	6.7532
C_{od} (€)	8012	2704	3215.6	1211.3	1010.25	41.515
C_{total} (€)	27,027	20,303	19922.8	20225	19810	19254

Table 5: Total Cost in distilled water and raw water heat exchanger (Case 3)

	Original design	GA	PSO	ABC	BBO	AIS
D_S (m)	0.387	0.62	0.018	1.002	0.55798	1.307
d_o (m)	0.019	0.016	0.0145	0.0103	0.01	0.0175
B (m)	0.305	0.44	0.423	0.354	0.5	0.2827
N_t	160	803	894	704	1565	2734
v_t (m/s)	1.76	0.68	0.74	0.36	0.898	0.17
Re_t	36,409	9487	9424	-	7804	698.25
P_{rt}	6.2	6.2	6.2	-	6.2	6.2
h_t (W/m^{2}k)	6558	6043	5618	4438	9180	101.96
s_t (m)	0.023	0.02	0.0187	-	0.0125	0.013
L (m)	4.88	1.548	1.45	2.4	1.133	1.04
Δp_t (Pa)	62812	3673	4474	2046	4176	176.80
f_t	0.023	0.031	0.03144	-	0.0337	0.079
a_s (m$^{2)}$	0.0236	0.0541	0.059	-	0.0558	0.056

d_e (m)	0.013	0.015	0.0103	-	0.0071	0.0173
v_s (m/s)	0.94	0.41	0.375	0.12	0.398	0.087
Re_s	16200	8039	4814	-	3515	3456
P_{rs}	5.4	5.4	5.4	-	5.4	5.4
h_s (W/m^{2}k)	5735	3476	4088	5608	4911	4878
f_s	0.337	0.374	0.403	-	0.42	0.428
Δp_s (Pa)	67684	4365	4271	2716	5917	2376
U (W/m^{2}k)	1471	1121	1176	1187	1384	474.76
A (m^2)	46.6	62.5	59.2	54.72	55.73	40.31
C_i (€)	16549	19163	18614	17893	18059	16067
C_o (€/yr)	4466	272	276	257.82	203.68	4.978
C_{od} (€)	27440	1671	1696	1584.2	1251	30.558
C_{total} (€)	43989	20834	20310	19428	19310	16098

Nomenclature

a_1	Numerical constant (€)
a_2	Numerical constant (€/m^2)
a_3	Numerical constant
a_s	Shell side pass area (m^2)
A	Heat exchanger surface area (m^2)
B	Baffle spacing (m)
C	Numerical constant
C_e	Energy cost (€/kW h)
C_i	Capital investment (€)
C	Clearance (m)
C_o	Annual operating cost (€)
C_{oD}	Total discounted operating cost (€)
C_p	Specific heat (J/kg K)
C_{tot}	Total annual cost (€)
c1	Numerical constant
d_e	Equivalent shell diameter (m)
d_i	Tube inside diameter (m)
d_o	Tube outside diameter (m)
D_s	Shell inside diameter (m)
F	Temperature difference correction factor
f_s	Shell side friction coefficient
f_t	Tube side friction coefficient
P	Pumping power (W)
Pr_s	Shell side Prandtl number
Pr_t	Tube side Prandtl number
Q	Heat duty (W)
Re_s	Shell side Reynolds number
Re_t	Tube side Reynolds number
R_{fs}	Shell side fouling resistance (m^2 K/W)
R_{ft}	Tube side fouling resistance (m^2 K/W)
S_t	Tube pitch (m)
T_{ci}	Cold fluid inlet temperature (K)
T_{co}	Cold fluid outlet temperature (K)
T_{hi}	Hot fluid inlet temperature (K)
T_{ho}	Hot fluid outlet temperature (K)
U	Overall heat transfer coefficient (W/m^2 K)
v_s	Shell side fluid velocity (m/s)
v_t	Tube side fluid velocity (m/s)
Δh	Heat transfer difference (W/m^2 K)
ΔP	Pressure drop (Pa)
$\Delta P_{tube\ elbow}$	Tube elbow Pressure drop (Pa)
$\Delta P_{tube\ length}$	Tube length Pressure drop (Pa)

Greek letters

H	Annual operating time (h/yr)	μ	Dynamic viscosity (Pa s)
h_s	Shell side convective coefficient (W/m^2 K)	ρ	Density (kg/m^3)
h_t	Tube side convective coefficient (W/m^2 K)	η	Overall pumping efficiency
i	Annual discount rate (%)		
k	Thermal conductivity (W/m^2 K)	Subscripts	
L	Tube length (m)	c	Cold stream
LMTD	Logarithmic Mean Temperature Difference (K)	e	Equivalent
m_s	Shell side mass flow (kg/s)	h	Hot stream
m_t	Tube side mass flow (kg/s)	i	Inlet
n	Number of tube passes	o	Outlet
n_1	Numerical constant	s	Shell side
n_y	Equivalent life (yr)	t	Tube side
N_t	Number of tubes	wt	Wall

REFERENCES

1. K.J.Bell, R.K. Shah, CRC Handbook of Thermal Engineering, CRC Press, Florida, 2000.
2. J.M.Coulson, R.K. Sinnot, J.F. Richardson, Chemical Engineering Design, Butterworth-Heinemann, Boston MA, 1996.
3. D.P.Dewitt, F.P. Incropera, Fundamentals of Heat and Mass Transfer, John Wiley, New York,1996.
4. R. Selbaş, Ö. Kızılkan, M. Reppich, A new design approach for shell-and-tube heat exchangers using genetic algorithms from economic point of view, Chemical Engineering and Processing: Process Intensification, 45(4) (2006) 268-275.
5. M. Fesanghary, E. Damangir, I. Soleimani, Design optimization of shell and tube heat exchangers using global sensitivity analysis and harmony search algorithm, Applied Thermal Engineering, 29(5–6) (2009) 1026-1031.
6. J. Taborek, Input Data and Recommended Practices, Heat Exchanger Design Handbook, Hemisphere Publishing Corporation, New York, 1983.
7. D.Q. Kern, Process Heat Transfer, McGraw-Hill ,New York, 1950.
8. K. Muralikrishna, U.V. Shenoy, Heat Exchanger Design Targets for Minimum Area and Cost, Chemical Engineering Research and Design, 78(2) (2000) 161-167.
9. A. Soršak, Z. Kravanja, MINLP retrofit of heat exchanger networks comprising different exchanger types, Computers & Chemical Engineering, 28(1–2) (2004) 235-251.
10. M.A.S.S. Ravagnani, J.A. Caballero, A MINLP Model for the Rigorous Design of Shell and Tube Heat Exchangers Using the Tema Standards, Chemical Engineering Research and Design, 85(10) (2007) 1423-1435.
11. A.C. Caputo, P.M. Pelagagge, P. Salini, Heat exchanger design based on economic optimisation, Applied Thermal Engineering, 28(10) (2008) 1151-1159.
12. J.M. Ponce-Ortega, M. Serna-González, A. Jiménez-Gutiérrez, Use of genetic algorithms for the optimal design of shell-and-tube heat exchangers, Applied Thermal Engineering, 29(2–3) (2009) 203-209.
13. I. Ozkol, G. Komurgoz, Determination of the Optimum Geometry of the Heat Exchanger Body Via A Genetic Algorithm, Numerical Heat Transfer, Part A: Applications, 48(3) (2005) 283-296.
14. G.N. Xie, B. Sunden, Q.W. Wang, Optimization of compact heat exchangers by a genetic algorithm, Applied Thermal Engineering, 28(8–9) (2008) 895-906.
15. André.L.H. Costa, E.M. Queiroz, Design optimization of shell-and-tube heat exchangers, Applied Thermal Engineering, 28(14–15) (2008) 1798-1805.
16. B. Khalifeh Soltan, M. Saffar-Avval, E. Damangir, Minimizing capital and operating costs of shell and tube condensers using optimum baffle spacing, Applied Thermal Engineering, 24(17–18) (2004) 2801-2810.
17. B.V. Babu, S.A. Munawar, Differential evolution strategies for optimal design of shell-and-tube heat exchangers, Chemical Engineering Science, 62(14) (2007) 3720-3739.

18. B. Allen, M. Savard-Goguen, L. Gosselin, Optimizing heat exchanger networks with genetic algorithms for designing each heat exchanger including condensers, Applied Thermal Engineering, 29(16) (2009) 3437-3444.

19. V.K. Patel, R.V. Rao, Design optimization of shell-and-tube heat exchanger using particle swarm optimization technique, Applied Thermal Engineering, 30(11–12) (2010) 1417-1425.

20. L.N.de. Castro, J.I. Timmis, Artificial immune systems as a novel soft computing paradigm, Soft Computing, 7(8) (2003) 526-544.

21. J.E. Hunt, D.E. Cooke, Learning using an artificial immune system, Journal of Network and Computer Applications, 19(2) (1996) 189-212.

22. V. Mariani, L. Santos Coelho, A. Duck, F. Guerra, R. Rao, Artificial Immune Network Approach with Beta Differential Operator Applied to Optimization of Heat Exchangers, Artificial Immune Systems, Springer Berlin Heidelberg, 2012, pp. 166-177.

23. R.M. Satheesh Kumar, P. Asokan, S. Kumanan, An artificial immune system-based algorithm to solve linear and loop layout problems in flexible manufacturing systems, International Journal of Product Development, 10(1) (2010) 165-179.

24. C.A.C. Coello, N.C. Cortés, Hybridizing a genetic algorithm with an artificial immune system for global optimization, Engineering Optimization, 36(5) (2004) 607-634.

25. H. Emma, T. Jon, Application areas of AIS: The past, the present and the future, Appl. Soft Comput., 8(1) (2008) 191-201.

26. A. Şencan Şahin, B. Kılıç, U. Kılıç, Design and economic optimization of shell and tube heat exchangers using Artificial Bee Colony (ABC) algorithm, Energy Conversion and Management, 52(11) (2011) 3356-3362.

27. A. Hadidi, A. Nazari, Design and economic optimization of shell-and-tube heat exchangers using biogeography-based (BBO) algorithm, Applied Thermal Engineering, 51(1–2) (2013) 1263-1272.

28. M.S.Peters,K.D.Timmerhaus, Plant Design and Economics for Chemical Engineers, McGraw-Hill ,New York, 1991.

Author' biography with Photo

K.Vetrivel kumar received B.E., degree in Mechanical Engineering from RVS College of Engineering and Technology, India and M.E., degree in Computer Aided Design from Alagappa Chettiar College of Engineering and Technology,Karaikudi, Anna University, India, in 2003 and 2007, respectively. Currently he is pursuing towards his Ph.D. degree in Anna University, India. Presently, he is an Associate Professor in the Department of Mechanical Engineering in SCAD Institute of Technology,Palladam, India. His research areas are Computational Fluid Dynamics, Heat exchangers design and optimization.

Dr.M. Saravanan holds an ME, PGDMM, DIS, PhD, MISTE, MIE, SMISME, FIIPE and MIIF. He is currently working as a Professor and Head of the Department of Mechanical Engineering, SSM Institute of Engineering and Technolgy, Dindigul, India. Previously, he was the Principal at Sri Subramanya College of Engineering and Technology, Palani, India. He received his PhD in the field of scheduling optimisation for various manufacturing systems from Anna University, India. His research interests are in the areas of scheduling for manufacturing systems, robotics, production planning, optimisation techniques, etc. He received his BE in Mechanical Engineering from Madurai Kamaraj University and ME in Production Engineering from Government College of Technology (Bharathiar University), Coimbatore, India. He has published more than 60 technical papers in the refereed international journals and more than 140 papers in the national and international conferences. He bagged three university awards and a state award for his tireless services in national service scheme for more than 12 years.